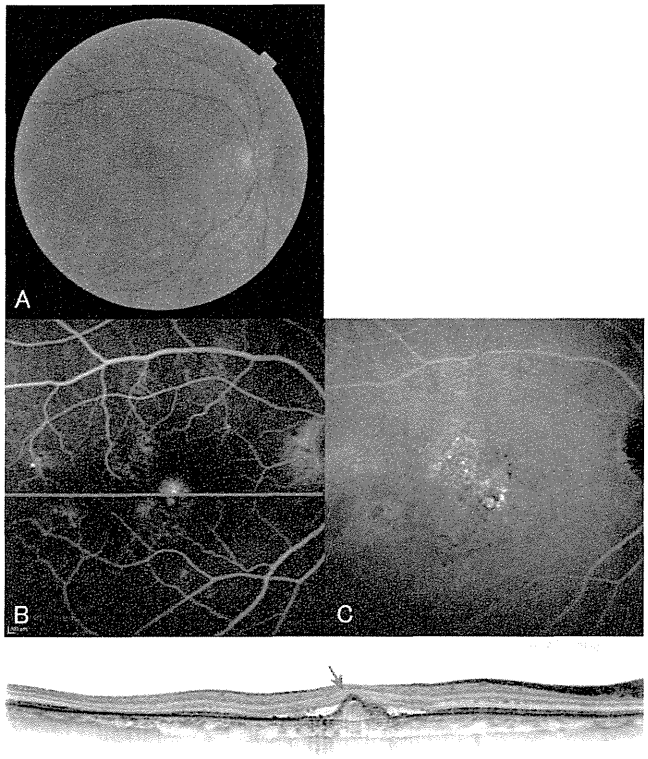

FIGURE 3. A CVH with type 1 CNV accompanied by a polypoidal lesion. (**A**) A 70-year-old man had visual impairment in the right eye (VA = 20/50). (**B**) An FA showing classic CNV with numerous dot-like hyperfluorescent spots. (**C**) Late-phase ICGA showing CVH (*arrows*) with a polypoidal lesion (*arrowhead*). (**D**) A horizontal OCT cross-sectional image reveals a sharply protruding retinal pigment epithelium, consistent with the polypoidal lesion seen in ICGA (*arrow*).

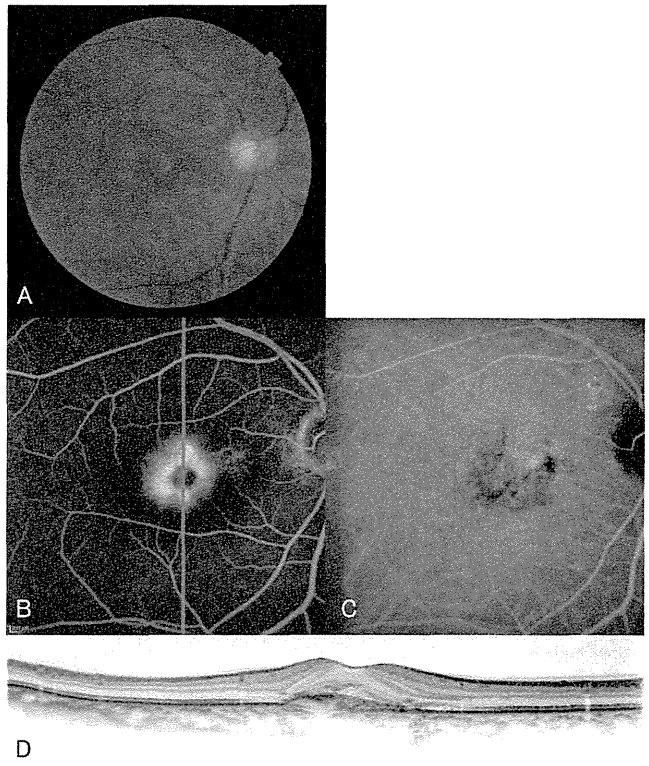

FIGURE 4. A CVH with both type 1 and 2 CNV. (**A**) A 72-year-old women had visual impairment in the right eye (VA = 20/32). (**B**) An FA showing classic CNV. (**C**) Late-phase ICGA showing typical CVH (*arrow*) and numerous hyperfluorescent spots. (**D**) A vertical OCT cross-sectional image reveals subfoveal type 1 and 2 CNV and a small amount of subretinal fluid.

lesions, but these differences were not statistically significant after adjusting for age.

Figure 5 shows the distribution of eyes with each feature in the context of the association between choroidal thickness and age. The solid line indicates the best-fit line (choroidal thickness [μm] = −4.10 × age [years] + 606) for data on the effect of choroidal thickness on age. Most eyes with only type 1 CNV, types 1 and 2 CNV, and type 1 CNV with polypoidal lesion belonged to patients who were ≥60 years old. Choroidal thickness in these eyes was distributed almost evenly along the regression line. Eyes with serous PED tended to belong to younger patients, while those with drusen tended to below to older patients.

Supplementary Table S1 summarizes patient characteristics of the two cohorts used as reference groups for genetic association testing. Tables 3 and 4 show results of the genetic association tests. Genotype distributions of *ARMS2* and *CFH* were significantly different in our subjects with CVH and type 1 CNV, and the Kyoto AMD cohort (*ARMS2*, $P = 1.4 \times 10^{-3}$; *CFH*, $P = 9.8 \times 10^{-3}$), but not with Nagahama control group (*ARMS2*, $P = 0.33$; *CFH*, $P = 0.82$). Power calculations revealed that for associations of the reported effect size (odds ratio [OR] = 2.7 for *ARMS2* and 0.42 for *CFH*),[32] we could have detected an association by 88.5% for *ARMS2* and 72.9% for *CFH*. Furthermore, genotype distribution of individuals with CVH and type 1 CNV was similar to Hapmap Japanese in Tokyo (Hapmap JPT, available in the public domain at http://hapmap.ncbi.nlm.nih.gov/index.html.en).

We also compared the genotype distributions in subjects with CVH and type 1 CNV to those in typical AMD cases or PCV cases from the Kyoto AMD cohort, summarized in Table 5. The subjects with CVH and type 1 CNV showed significantly different genotype distributions from those with typical AMD or PCV, respectively.

Discussion

To date and to our knowledge, there is no available information on the prevalence of CVH in the cohort study. In the current study, CVH was seen in 26.1%. However, data were collected through a retrospective review of medical records of consecutive patients examined with ICGA, performed because of macular disease suspicions. Because asymptomatic subjects rarely visit the clinic, we may have overestimated the CVH prevalence. On the other hand, ICGA often reveals CVH in the asymptomatic fellow eye of patients with unilateral CSC. Therefore, the prevalence of asymptomatic CVH may have been higher than we assumed.

In the current study, 175 of 227 eyes (77.4%) with CVH had no evidence of CNV, but type 1 CNV in the macular area was confirmed in 51 eyes (22.5%). Pure type 2 CNV (with no type 1 CNV) was seen in only one eye (0.4%). Therefore, we estimated that 22.6% (95% confidence interval [CI], 17.6%–28.9%) of eyes with CVH also had CNV. The true prevalence of type 1 CNV in eyes with CVH would be lower because of the selection bias our inclusion criteria introduced. Nevertheless, type 1 CNV is not a rare complication in eyes with CVH based on the estimates of the current study.

Investigative Ophthalmology & Visual Science

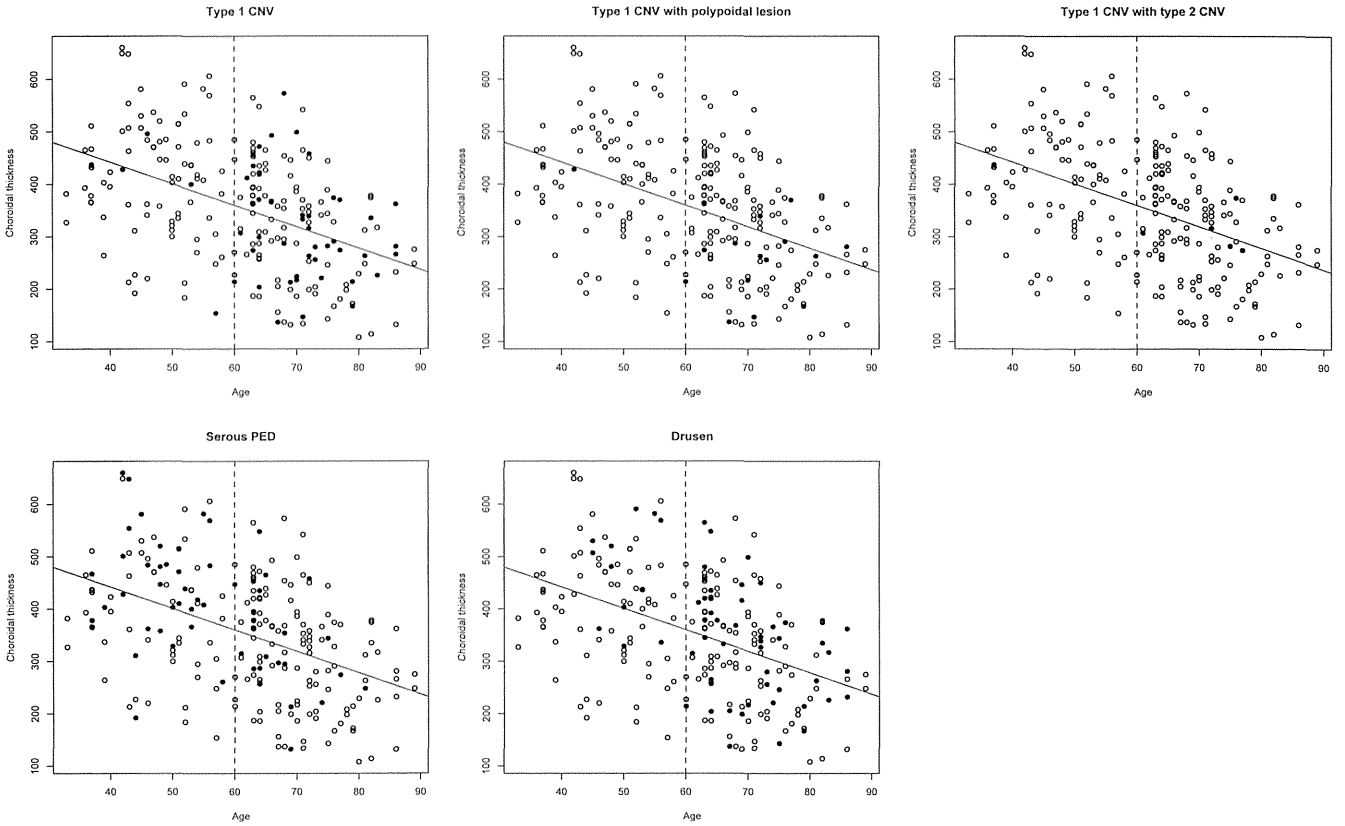

Figure 5. Choroidal thickness versus patient age. All eyes with CVH were plotted. Each *solid line* represents the best-fit line of how choroidal thickness is affected by age (choroidal thickness [μm] = −4.10 × age [years] + 606). Each *broken line* is a line of a 60-year-old. (**A**) Eyes with pure type 1 CNV are highlighted in *closed circles*. (**B**) Eyes with type 1 CNV and polypoidal lesions are highlighted in *closed circles*. (**C**) Eyes with type 1 and 2 CNV are highlighted in *closed circles*. (**D**) Eyes with serous pigment epithelial detachment are highlighted in *closed circles*. (**E**) Eyes with drusen are highlighted in *closed circles*.

The mean age of patients with type 1 CNV was significantly higher than in patients without CNV. Although the proportion of eyes with a serous PED or drusen, along with choroidal thickness, tended to be higher in eyes with type 1 CNV, these differences were not statistically significant after age adjustments were made. Spaide et al.[4] previously reported that older patients with CSC had a lower VA, and were more likely to have diffuse retinal pigment epitheliopathy, bilateral involvement, and secondary CNV than their younger counterparts. Although most eyes with classic CSC also have CVH in younger patients, they rarely develop CNV. It is possible that some patients with CVH go on to develop CNV at an older age.

Of the 51 eyes with type 1 CNV, polypoidal lesions and type 2 CNV also were present in 33.3% and 11.8% of eyes, respectively. Several previous reports also have indicated that the choroid is thicker in eyes with PCV than in eyes with AMD.[33–35] On the other hand, Jirarattanasopa et al.[12] reported that choroidal thickness was significantly greater in eyes with PCV and no CVH (225.7 μm) than in eyes with AMD and no CVH (158.9 μm). They also reported that choroidal thickness is not different in eyes with CVH and AMD (278.2 μm), and in eyes with CVH and PCV (283.4 μm). In our patients with CVH, eyes with polypoidal lesions (268.5 μm) had a thinner choroid than those with pure type 1 CNV (353.0 μm). However, choroidal thickness still was greater than in healthy eyes, as reported previously in patients averaging 64.6 years of age (203.6 μm)[36] and in AMD (158.9 μm) or PCV (225.7μm) eyes with no CVH.[12] Therefore, CVH is associated primarily with an increase in choroidal thickness.

Table 3. Comparison of A69S Genotype Frequency

	GG	GT	TT	T Allele Frequency	*P* Value*
AMD	302	587	620	0.605	1.4×10^{-3}
Hyperpermeability + type 1 CNV	15	19	8	0.417	Reference
Nagahama control	1312	1499	435	0.365	0.33†
Hapmap JPT	15	21	9	0.433	0.83

* Indicates χ^2 test for trend.

† Indicates statistical power = 88.5% (assuming OR = 2.7, minor allele frequency = 0.40).

Table 4. Comparison of the I62V Genotype Frequency

	GG	GA	AA	A Allele Frequency	*P* Value*
AMD	856	578	121	0.264	9.8×10^{-3}
Hyperpermeability + type 1 CNV	16	19	7	0.393	Reference
Nagahama control	1162	1538	546	0.405	0.82†
Hapmap JPT	16	22	6	0.386	0.93

* Indicates χ^2 test for trend.

† Indicates statistical power = 72.9% (assuming OR = 0.42, minor allele frequency = 0.40).

TABLE 5. Differences of Genotype Distributions Against Typical AMD or PCV

	ARMS2 A69S						CFH I62V					
	GG	GT	TT	T Allele Frequency	OR (95% CI)	*P* Value*	GG	GA	AA	A Allele Frequency	OR (95% CI)	*P* Value*
CVH + type 1 CNV	15	19	8	0.417	-	-	16	19	7	0.393		-
PCV	186	310	282	0.562	1.79 (1.15-2.80)	0.017	438	294	67	0.268	0.57 (0.36-0.89)	0.015
Typical AMD	111	272	308	0.645	2.52 (1.61-3.94)	1.0×10^{-4}	402	270	47	0.253	0.52 (0.33-0.82)	4.9×10^{-3}

* χ^2 test for trend.

Recently, Fung et al.[22] reported that, compared to patients with type 1 neovascularization secondary to AMD, patients with type 1 CNV associated with CSC are more likely to be younger and male, have thicker choroids, and have polypoidal lesions. Although it is rather difficult to compare our findings to those of this report because of inclusion criteria differences, choroidal thickness in our patients (323.5 μm) was compatible with that measured in eyes with "CNV secondary to CSC" (356.5 μm). In addition, the rate of concomitant polypoidal lesions was comparable between our study (33.3%) and that of Fung et al.[22] (36%).

Both *ARMS2* and *CFH* generally are thought as the two most important SNPs associated with the development of AMD and PCV in Caucasian and Japanese populations.[12,24-27] In the current study, genetic association analysis showed that the genetic background of patients with type 1 CNV and CVH was different from that of patients with AMD. Statistical testing showed that the probability of such a deviation occurring by chance is 0.14% and 0.98% for the *ARMS2* and *CFH* gene variations, respectively. Their different genetic background from those of typical AMD cases and PCV cases (shown in Table 5) also is important; it raises the possibility that type 1 CNV with CVH is different not only from typical AMD, but also PCV. Furthermore, no significant differences were observed in genotype between patients with type 1 CNV and CVH and Japanese controls. Because the statistical powers of these association tests were adequate (88.5% and 72.9% for *ARMS2* and *CFH*, respectively), it is unlikely that a false-negative occurred, especially for the *ARMS2* gene variation.

The current result of the *CFH* association test is supported by a previous report[12] that compared the *CFH* I62V genotype between patients with AMD and CVH, and patients with AMD and no CVH. This report showed that patients with AMD and CVH had a more similar genotype distribution (A allele frequency of 34%) to Japanese controls than did patients with AMD and no CVH (A allele frequency of 24%). Because *ARMS2* or *CFH* genotyping is not the gold standard in diagnosing AMD, we cannot clearly distinguish AMD from CSC by simply examining the *ARMS2* or *CFH* genotypes. However, judging from the two major genes (*ARMS2* and *CFH*), CNV with CVH has a different genetic background than CNV associated with AMD, and has similar genetic background as control subjects.

Yannuzzi et al.[37] previously published a report on 13 patients initially suspected of having CSC, but ultimately were diagnosed with PCV. Because none of these cases also had CVH, we believe that these eyes were likely to be PCV from the start. Based on accumulating ICGA and OCT evidence, it generally is believed that CVH is a principal pathophysiologic abnormality underlying CSC. Since Sasahara et al.[13] reported an association between CVH and PCV, various investigators have examined the clinical features of these eyes and thought that these eyes had AMD or PCV that was accompanied by CVH.[12,14,15,33,38] However, in a recent report by Fung et al.,[22] CVH was attributed to CNV or polypoidal lesions secondary to CSC. Unfortunately, whether CNV with CVH originally began as AMD or as CSC remains controversial. However, our study results added further insight to this argument, from the genetic point of view.

This study has various limitations. First, this study is a retrospective, hospital-based study. Ideally, we would have enrolled consecutive subjects from a long-term, prospective, population-based cohort. However, because it is ethically questionable to perform ICGA on healthy subjects, accurately estimating CVH prevalence in the general population would have been difficult. Second, eyes were determined to have CVH only if independent diagnoses of 2 retinal specialists agreed. This increased diagnostic specificity for CVH, but decreased the sensitivity, and marginal cases had to be ignored. Additional objective criteria or diagnostic methods are needed to eliminate subjective interpretation of CVH in the further studies. Third, we only examined the two most important SNPs associated with the development of AMD and PCV (*ARMS2* and *CFH*). Genotypes of many other diseases susceptible to SNPs might provide further understanding of the current issues. Fourth is the quality of controls in the genetic association tests. If the prevalence of CVH with type 1 CNV was high in the general population, then the statistical power of the genetic association test is lower than we estimated. Although we can assume that the CVH with type 1 CNV prevalence in the general population is not high based on the low prevalence of CNV[30] and CSC,[39,40] we must interpret the negative associations with caution. Finally, this is a cross-sectional study, and lacks an investigation of treatment efficacy and long-term visual prognosis. These should be explored in future prospective, long-term studies.

In summary, the current study describes the clinical characteristics of CNV that is seen in eyes with CVH. Type 1 CNV was seen more frequently than it was thought, and they sometimes accompanied type 2 CNV or polypoidal lesions. Additionally, the genetic background of these patients was different from AMD patients, but rather similar to the general Japanese population, suggesting that "CNV with CVH" might be one cluster of CNV distinguished from AMD.

Acknowledgments

The authors thank Takeo Nakayama (Department of Health Informatics, Kyoto University School of Public Health, Kyoto, Japan), Akihiro Sekine (Department of Genome Informatics, Kyoto University School of Public Health, Kyoto, Japan), Shinji Kosugi (Department of Medical Ethics, Kyoto University School of Public Health, Kyoto, Japan), Yasuharu Tabara (Center for Genomic Medicine, Graduate School of Medicine, Kyoto University), and Ryo Yamada (Center for Genomic Medicine, Graduate School of Medicine, Kyoto University) for their efforts with the Nagahama study.

The authors alone are responsible for the content and writing of the paper.

Disclosure: **M. Miyake**, None; **A. Tsujikawa**, Pfizer (F); **K. Yamashiro**, None; **S. Ooto**, None; **A. Oishi**, None; **H. Tamura**,

None; **I. Nakata**, None; **F. Matsuda**, None; **N. Yoshimura**, Topcon Corporation (F), Nidek (F), Canon (F)

References

1. Guyer DR, Puliafito CA, Mones JM, et al. Digital indocyanine-green angiography in chorioretinal disorders. *Ophthalmology.* 1992;99:287–291.
2. Piccolino FC, Borgia L. Central serous chorioretinopathy and indocyanine green angiography. *Retina.* 1994;14:231–242.
3. Spaide RF, Yannuzzi LA, Slakter JS, et al. Indocyanine green videoangiography of idiopathic polypoidal choroidal vasculopathy. *Retina.* 1995;15:100–210.
4. Spaide RF, Campeas L, Haas A, et al. Central serous chorioretinopathy in younger and older adults. *Ophthalmology.* 1996;103:2070–2079. discussion 9–80.
5. Lafaut BA, Salati C, Priem H, De Laey JJ. Indocyanine green angiography is of value for the diagnosis of chronic central serous chorioretinopathy in elderly patients. *Graefes Arch Clin Exp Ophthalmol.* 1998;236:513–521.
6. Tsujikawa A, Ojima Y, Yamashiro K, et al. Punctate hyperfluorescent spots associated with central serous chorioretinopathy as seen on indocyanine green angiography. *Retina.* 2010;30:801–809.
7. Guyer DR, Yannuzzi LA, Slakter JS, et al. Digital indocyanine green videoangiography of central serous chorioretinopathy. *Arch Ophthalmol.* 1994;112:1057–1062.
8. Piccolino FC, Borgia L, Zinicola E, Zingirian M. Indocyanine green angiographic findings in central serous chorioretinopathy. *Eye.* 1995;9:324–332.
9. Spaide RF, Hall L, Haas A, et al. Indocyanine green videoangiography of older patients with central serous chorioretinopathy. *Retina.* 1996;16:203–213.
10. Menchini U, Virgili G, Lanzetta P, Ferrari E. Indocyanine green angiography in central serous chorioretinopathy. ICG angiography in CSC. *Int Ophthalmol.* 1997;21:57–69.
11. Iida T, Kishi S, Hagimura N, Shimizu K. Persistent and bilateral choroidal vascular abnormalities in central serous chorioretinopathy. *Retina.* 1999;19:508–512.
12. Jirarattanasopa P, Ooto S, Nakata I, et al. Choroidal thickness, vascular hyperpermeability, and complement factor H in age-related macular degeneration and polypoidal choroidal vasculopathy. *Invest Ophthalmol Vis Sci.* 2012;53:3663–3672.
13. Sasahara M, Tsujikawa A, Musashi K, et al. Polypoidal choroidal vasculopathy with choroidal vascular hyperpermeability. *Am J Ophthalmol.* 2006;142:601–607.
14. Koizumi H, Yamagishi T, Yamazaki T, Kinoshita S. Relationship between clinical characteristics of polypoidal choroidal vasculopathy and choroidal vascular hyperpermeability. *Am J Ophthalmol.* 2013;155:305–313.
15. Maruko I, Iida T, Sugano Y, et al. Subfoveal retinal and choroidal thickness after verteporfin photodynamic therapy for polypoidal choroidal vasculopathy. *Am J Ophthalmol.* 2011;151:594–603.
16. Quin G, Liew G, Ho IV, et al. Diagnosis and interventions for central serous chorioretinopathy: review and update. *Clin Exp Ophthalmol.* 2013;41:187–200.
17. Mudvari SS, Goff MJ, Fu AD, et al. The natural history of pigment epithelial detachment associated with central serous chorioretinopathy. *Retina.* 2007;27:1168–1173.
18. Cooper BA, Thomas MA. Submacular surgery to remove choroidal neovascularization associated with central serous chorioretinopathy. *Am J Ophthalmol.* 2000;130:187–191.
19. Chan WM, Lam DS, Lai TY, et al. Treatment of choroidal neovascularization in central serous chorioretinopathy by photodynamic therapy with verteporfin. *Am J Ophthalmol.* 2003;136:836–845.
20. Yang CS, Chen KC, Lee SM, Lee FL. Photodynamic therapy in the treatment of choroidal neovascularization complicating central serous chorioretinopathy. *J Chin Med Assoc.* 2009;72:501–505.
21. Ahuja RM, Downes SM, Stanga PE, et al. Polypoidal choroidal vasculopathy and central serous chorioretinopathy. *Ophthalmology.* 2001;108:1009–1010.
22. Fung AT, Yannuzzi LA, Freund KB. Type 1 (sub-retinal pigment epithelial) neovascularization in central serous chorioretinopathy masquerading as neovascular age-related macular degeneration. *Retina.* 2012;32:1829–1837.
23. Spaide RF, Koizumi H, Pozzoni MC. Enhanced depth imaging spectral-domain optical coherence tomography. *Am J Ophthalmol.* 2008;146:496–500.
24. Hageman GS, Anderson DH, Johnson LV, et al. A common haplotype in the complement regulatory gene factor H (HF1/CFH) predisposes individuals to age-related macular degeneration. *Proc Natl Acad Sci U S A.* 2005;102:7227–7232.
25. Mori K, Gehlbach PL, Kabasawa S, et al. Coding and noncoding variants in the CFH gene and cigarette smoking influence the risk of age-related macular degeneration in a Japanese population. *Invest Ophthalmol Vis Sci.* 2007;48:5315–5319.
26. Hayashi H, Yamashiro K, Gotoh N, et al. CFH and ARMS2 variations in age-related macular degeneration, polypoidal choroidal vasculopathy, and retinal angiomatous proliferation. *Invest Ophthalmol Vis Sci.* 2010;51:5914–5919.
27. Rivera A, Fisher SA, Fritsche LG, et al. Hypothetical LOC387715 is a second major susceptibility gene for age-related macular degeneration, contributing independently of complement factor H to disease risk. *Hum Mol Genet.* 2005;14:3227–3236.
28. Schmidt S, Hauser MA, Scott WK, et al. Cigarette smoking strongly modifies the association of LOC387715 and age-related macular degeneration. *Am J Hum Genet.* 2006;78:852–864.
29. Yoshimura K, Nakayama T, Sekine A, et al. B-type natriuretic peptide as an independent correlate of nocturnal voiding in Japanese women. *Neurourol Urodyn.* 2012;31:1266–1271.
30. Nakata I, Yamashiro K, Nakanishi H, et al. Prevalence and characteristics of age-related macular degeneration in the Japanese population: the Nagahama study. *Am J Ophthalmol.* 2013;156:1002–1009.
31. Nakata I, Yamashiro K, Kawaguchi T, et al. Association between the cholesteryl ester transfer protein gene and polypoidal choroidal vasculopathy. *Invest Ophthalmol Vis Sci.* 2013;54;6068–6073.
32. Fritsche LG, Chen W, Schu M, et al. Seven new loci associated with age-related macular degeneration. *Nat Genet.* 2013;45:433–439.
33. Koizumi H, Yamagishi T, Yamazaki T, et al. Subfoveal choroidal thickness in typical age-related macular degeneration and polypoidal choroidal vasculopathy. *Graefes Arch Clin Exp Ophthalmol.* 2011;249:1123–1128.
34. Baja ES, Schwartz JD, Wellenius GA, et al. Traffic-related air pollution and QT interval: modification by diabetes, obesity, and oxidative stress gene polymorphisms in the normative aging study. *Environ Health Perspect.* 2010;118:840–846.
35. Kim SW, Oh J, Kwon SS, et al. Comparison of choroidal thickness among patients with healthy eyes, early age-related maculopathy, neovascular age-related macular degeneration, central serous chorioretinopathy, and polypoidal choroidal vasculopathy. *Retina.* 2011;31:1904–1911.
36. Hirata M, Tsujikawa A, Matsumoto A, et al. Macular choroidal thickness and volume in normal subjects measured by swept-source optical coherence tomography. *Invest Ophthalmol Vis Sci.* 2011;52:4971–4978.

Investigative Ophthalmology & Visual Science

37. Yannuzzi LA, Freund KB, Goldbaum M, et al. Polypoidal choroidal vasculopathy masquerading as central serous chorioretinopathy. *Ophthalmology.* 2000;107:767–777.
38. Chung SE, Kang SW, Lee JH, Kim YT. Choroidal thickness in polypoidal choroidal vasculopathy and exudative age-related macular degeneration. *Ophthalmology.* 2011;118:840–845.
39. Tsai DC, Chen SJ, Huang CC, et al. Epidemiology of idiopathic central serous chorioretinopathy in Taiwan, 2001-2006: a population-based study. *PloS One.* 2013;8:e66858.
40. Kitzmann AS, Pulido JS, Diehl NN, et al. The incidence of central serous chorioretinopathy in Olmsted County, Minnesota, 1980-2002. *Ophthalmology.* 2008;115:169–173.

Investigative Ophthalmology & Visual Science

SCIENTIFIC REPORTS

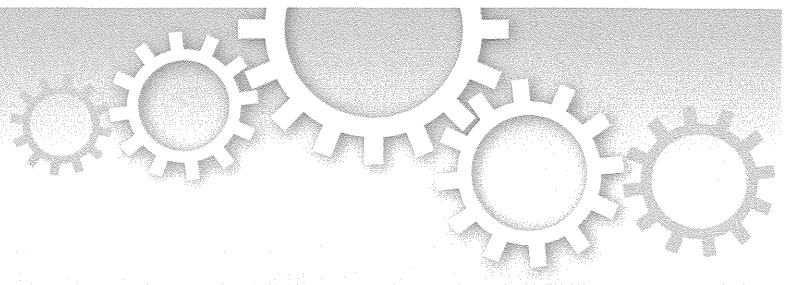

OPEN

SUBJECT AREAS:
DRUG DISCOVERY
CELL DEATH

Received
30 December 2013

Accepted
18 July 2014

Published
6 August 2014

Correspondence and requests for materials should be addressed to A.K. (kakizuka@lif.kyoto-u.ac.jp)

Novel VCP modulators mitigate major pathologies of rd10, a mouse model of retinitis pigmentosa

Hanako Ohashi Ikeda[1,2], Norio Sasaoka[2], Masaaki Koike[2], Noriko Nakano[1], Yuki Muraoka[1], Yoshinobu Toda[3], Tomohiro Fuchigami[4], Toshiyuki Shudo[1,2,4], Ayana Iwata[2], Seiji Hori[2], Nagahisa Yoshimura[1] & Akira Kakizuka[2]

[1]Department of Ophthalmology and Visual Sciences, Kyoto University Graduate School of Medicine, Kyoto 606-8501, Japan, [2]Laboratory of Functional Biology, Kyoto University Graduate School of Biostudies, Kyoto 606-8501, Japan, [3]Center for Anatomical Studies, Kyoto University Graduate School of Medicine, Kyoto 606-8501, Japan, [4]Daito Chemix, Ishibashi-cho Fukui-city Fukui 910-3137, Japan.

Neuroprotection may prevent or forestall the progression of incurable eye diseases, such as retinitis pigmentosa, one of the major causes of adult blindness. Decreased cellular ATP levels may contribute to the pathology of this eye disease and other neurodegenerative diseases. Here we describe small compounds (Kyoto University Substances, KUSs) that were developed to inhibit the ATPase activity of VCP (valosin-containing protein), the most abundant soluble ATPase in the cell. Surprisingly, KUSs did not significantly impair reported cellular functions of VCP but nonetheless suppressed the VCP-dependent decrease of cellular ATP levels. Moreover, KUSs, as well as exogenous ATP or ATP-producing compounds, e.g. methylpyruvate, suppressed endoplasmic reticulum stress, and demonstrably protected various types of cultured cells from death, including several types of retinal neuronal cells. We then examined their *in vivo* efficacies in rd10, a mouse model of retinitis pigmentosa. KUSs prevented photoreceptor cell death and preserved visual function. These results reveal an unexpected, crucial role of ATP consumption by VCP in determining cell fate in this pathological context, and point to a promising new neuroprotective strategy for currently incurable retinitis pigmentosa.

Despite recent advances in the development of new drugs, there remain many incurable disorders, e.g. neurodegenerative diseases, ischemic diseases, and chronic inflammation, in which the major pathology in the affected organs is early cell death, which occurs long before the death of the individual. Indeed, currently no drug is available to prevent such early cell death *in vivo*. If such drugs were available, many of these disorders, if not all, might be prevented or delayed. In the 1990s, due to a growing, but still imperfect, understanding of the molecular bases of apoptotic cell death, caspase inhibitors were developed and were heralded as miracle drugs, but they were ineffective in preventing cell death *in vivo*. This might be explained as follows: caspases determine how cells die but are unable to affect the commitment to cell death. Thus, drugs that could delay or prevent the commitment to cell death have been actively pursued.

Retinitis pigmentosa, which is caused by a gradual degeneration and loss of photoreceptors, is another intractable eye disease, and more than 1.5 million patients suffer from progressive visual deterioration with this disorder. Clinical trials using a neurotrophic factor have been initiated[1]. In retinitis pigmentosa, involvement of endoplasmic reticulum (ER) stress has been proposed[2,3]. Thus, new drugs or compounds with ER stress-reducing activities may prove to be neuroprotective, and are thus worth investigating for the treatment or prevention of retinitis pigmentosa.

We have long been working to elucidate the molecular bases of polyglutamine diseases, as informative models for neurodegeneration. We and other research groups produced several lines of evidence that implicate valosin-containing protein (VCP), an AAA (ATPases Associated with diverse cellular Activities)-type ATPase with ubiquitous expression, as a major player causing neurodegeneration. It is notable that VCP is highly conserved among species; its amino acid sequences are completely identical among mouse, rat, and human, and 84% identical between human and *Drosophila*[4]. We first assumed that specific cellular genes are involved in the pathogenesis of polyglutamine diseases, and thus had established *Drosophila* models of polyglutamine diseases

for genetic analyses. Mutant screening revealed that *Ter94* loss-of-function alleles mitigated polyglutamine-induced eye degeneration[4]. Conversely, overexpression of wild-type *Ter94* enhanced the polyglutamine-induced eye degeneration[4]. Since the mammalian *Ter94* ortholog is *VCP*, these results raised the possibility that VCP is involved in the pathogenesis of human neurodegenerative diseases[5]. Consistent with this possibility, VCP mutations were identified that are causative for IBMPFD (inclusion body myopathy associated with Paget disease of bone and frontotemporal dementia)[6], a human hereditary disease with dementia, or for rare cases of familial amyotrophic lateral sclerosis (ALS)[7]. In our evaluation, all tested pathogenic VCPs possessed elevated ATPase activities, as compared with wild-type VCP[8], indicating that the constitutive elevation of its ATPase activity may be pathogenic.

These lines of evidence suggested that inhibitors of the ATPase activity of VCP could protect neuronal cells. In addition to its ATPase activity, however, many cellular functions of VCP have been proposed[9–11], e.g., proteasome-mediated protein degradation, endoplasmic reticulum-associated degradation (ERAD), cell cycle control, membrane fusion, maintenance of the Golgi apparatus, protein trafficking, autophagy, genomic DNA surveillance, etc., some of which are crucial for cell survival. Indeed, VCP knockdown and overexpression of dominant-negative forms of VCP showed toxicity in cultured cells[12,13]. DBeQ, a recently reported VCP inhibitor (*in vitro* IC_{50} (half maximal inhibitory concentration) 1 μM)[14], also showed cellular toxicity. Given that VCP has multiple cellular functions, some of them would require ATP hydrolysis and others would not. Thus, it is a challenge to find small compounds that can inhibit or reduce the ATPase activity of VCP without incurring the general toxicity caused by loss of crucial cellular functions of VCP.

Results

KUSs inhibited VCP ATPase activity but not VCP cellular functions. In our search for novel VCP ATPase inhibitors, we found that a naphthalene derivative can inhibit the ATPase activity of VCP with no apparent toxicity at 10 μM on cultured cells. Based on the chemical structure, about two hundred compounds were newly synthesized and named KUSs (Kyoto University substances). Some of them, e.g. KUS31, 69, 94, 121, and 187, clearly inhibited the ATPase activity of recombinant VCP *in vitro* with IC_{50} values ranging from approximately 100 nM to 1 μM (Fig. 1a). These IC_{50} values were equivalent to or much lower than that of DBeQ[14], whose reported IC_{50} is 1 μM (Supplementary Fig. 1). It is notable that KUSs very mildly inhibited the ATPase activity of N-ethylmaleimide-sensitive fusion protein (NSF) (Fig. 1b), whose structure is most closely related with that of VCP.

We then examined the effect of KUS31, 69, 94, 121, and 187 on VCP functions in cultured cells. We also used DBeQ as a reference compound. As reported, DBeQ induced accumulation of ubiquitinated proteins, ER stress, autophagy, and eventually cell death (Fig. 1c and d). Surprisingly, these compounds did not induce any of these phenotypes (Fig. 1c and d). These results clearly indicated that ATPase inhibition by KUS31, 69, 94, 121, and 187 (referred to as "KUSs" hereafter, for simplicity) did not interfere with reported cellular VCP functions (referred to as "VCP functions" hereafter), indicating that VCP functions do not necessarily require its ATPase activity (see Discussion).

KUSs protected cells under ER stress-inducing conditions. Additionally, KUSs protected cells from several cell death-inducing insults. For example, when HeLa cells were cultured under low glucose conditions (0.2 g/l of glucose), all cells died within several days (Fig. 2a). However, when KUSs were present in the media, they prevented cell death (Fig. 2a and b). Protective effects were also observed when HeLa cells were treated with tunicamycin (Tm) (Fig. 2c), or when HEK293 cells were subjected to serum-free conditions (Fig. 2d). These protective effects of KUSs were dose-dependent, as exemplified by KUS121 (Fig. 2e). These data clearly implied that inhibition of VCP ATPase activity by KUSs could protect cells from several cell death-inducing insults.

Tunicamycin treatment and glucose starvation are known to cause ER stress and to lead to cell death. C/EBP-homologous protein (CHOP) is a core mediator of ER stress-induced cell death, and is upregulated during ER stress[15]. Indeed, KUSs suppressed the expression of CHOP in tunicamycin-treated HeLa cells (Fig. 2f). KUSs also suppressed the expression of 78 kDa glucose-regulated protein (Grp78), another ER stress marker[16], in the tunicamycin-treated cells. Next, we examined Akt (serine/threonine-protein kinase) activation by examining its phosphorylation at Ser473, which has been reported to be necessary and sufficient for cell survival[17]. The phosphorylated Akt signal nearly disappeared in cells treated with tunicamycin, but was clearly detected in cells treated with tunicamycin and KUSs (Fig. 2f). These data indicate that KUSs could suppress ER stress and promote cell survival, which was evidenced by Akt being in an activated state.

Because VCP is a major ATPase in cells, we then examined the contribution of VCP to total ATPase activities in clarified whole cell lysates, and found that VCP appeared to contribute to approximately 20%–40% of the total collective ATPase activity, depending on the cell types and culture conditions (an example is provided in Fig. 3a). In neuronally differentiated PC12 cells, for example, 100 nM and 1 μM KUS121, as well as KUS187, significantly lowered the total ATPase activity (approximately 20% and 40% for both concentrations, respectively) (Fig. 3a). Given that the IC_{50} values of KUS121 and KUS187 on recombinant VCP were around 200 ~ 300 nM (Fig. 1a), these data implied that the ATPase activity of VCP contributed to as much as 40% of the total soluble ATPase activities in the cell lysate. This estimation was further supported by the observation that 1 μM KUS94 (IC_{50} is 1 μM) also showed approximately 20% suppression of the soluble ATPase activities (Fig. 3a). Consistent with the inability of KUS11 to inhibit the ATPase of VCP *in vitro* (IC_{50} is more than 100 μM), KUS11 did not show any significant inhibition of total ATPase activity in the clarified lysates (Fig. 3a).

We next examined whether KUSs altered cellular ATP levels. At 20 hours after a change to low glucose medium (0.25 g/l), glucose concentrations in the medium approached zero, and ATP levels in the cells (control cells) significantly decreased (Fig. 3b). In contrast, ATP levels in the cells with low glucose medium plus KUSs remained significantly higher than those in the control cells (Fig. 3b and Supplementary Fig. 2a). In addition, in KUS-treated cells, the ratio of ATP to ADP was higher than in the control cells (Supplementary Fig. 2b). These data indicate that KUSs suppress consumption of ATP in cells under stress conditions. Interestingly, acetyl-CoA levels in the KUS-treated cells were significantly lower than those in the control cells (Fig. 3c and Supplementary Fig. 2c), suggesting the possibility that KUSs may induce a metabolic shift from a glycolytic pathway to mitochondrial pathways to produce ATP. This possibility remains to be clarified. The low levels of acetyl-CoA might also contribute to protect cells from cell death, as reported recently[18].

KUSs and exogenous ATP both prevented ER stress in cultured cells. It has long been believed that ER stress is induced by the accumulation of misfolded proteins, or protein aggregates, in the ER[19–21]. We recently identified laminin γ1 as an aggregation-prone protein in the ER. We therefore examined laminin γ1 as an indicator of ER-stress in tunicamycin-treated cells. By immunocytochemical analyses, expression of laminin γ1 was observed in a diffuse pattern throughout the ER in normal cells (Control in Fig. 4a). When cells were treated with tunicamycin, laminin γ1 formed clear aggregates (DMSO in Fig. 4a). However, not only 50 μM KUSs (KUS69, 94, 121, and 187) but also 1 mM ATP treatments clearly prevented the aggregation of laminin γ1 (Fig. 4a). Consistent with these results,

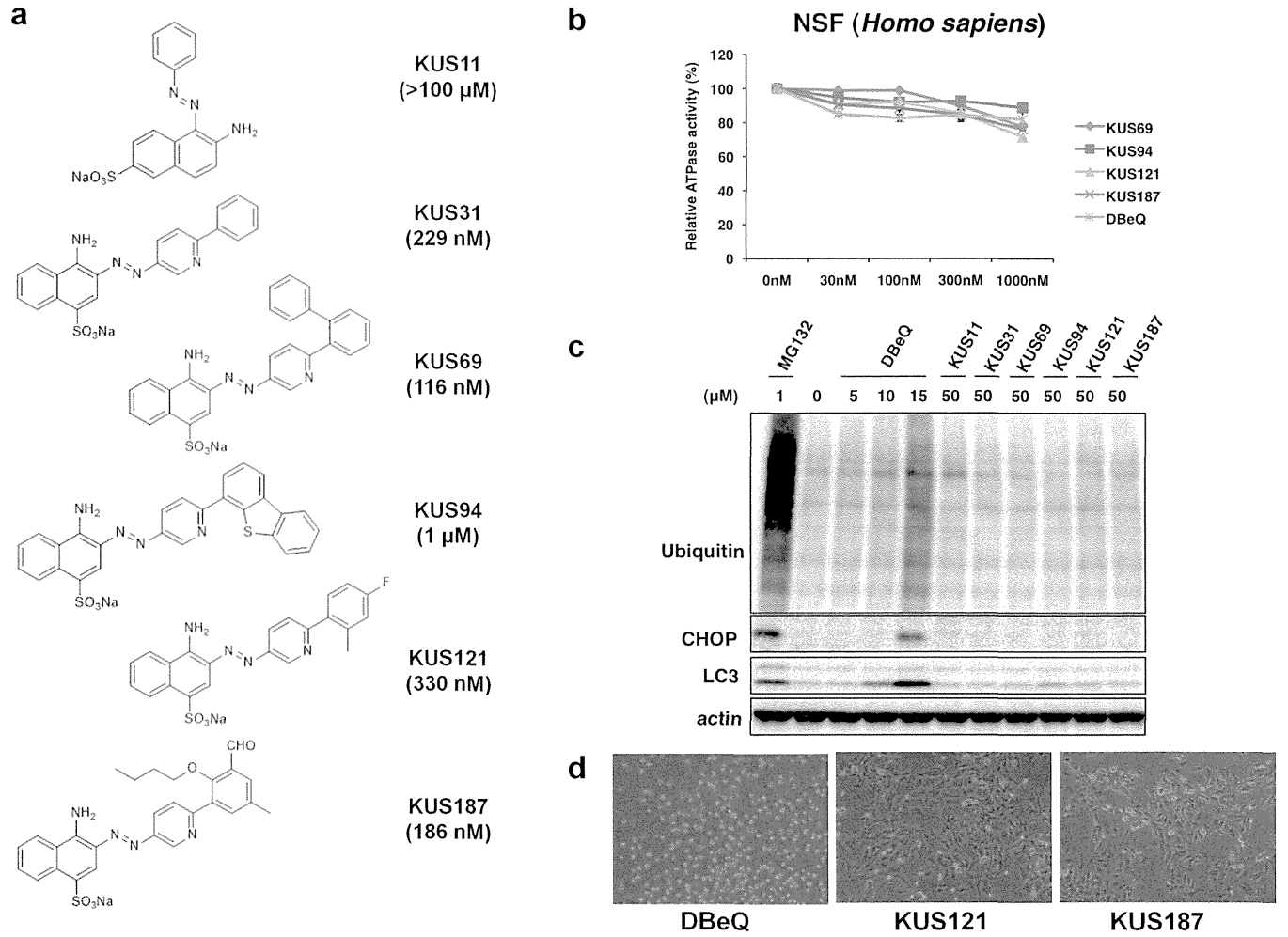

Figure 1 | Structures and characterization of KUSs, novel VCP modulators. (a) Structures and IC_{50} values of KUS11, KUS31, KUS69, KUS94, KUS121, and KUS187. Note that KUS11 did not inhibit the ATPase activity of recombinant VCP, and it did not share a common structure with the other KUSs. (b) ATPase activity assays of recombinant human NSF, comparing KUSs and DBeQ. (c) Immunoblot analysis of ubiquitinated proteins, an ER stress marker (CHOP), and an autophagy indicator (LC3), comparing KUSs and DBeQ. As a control, MG132, a proteasome inhibitor, was used for the analysis. Actin served as a loading control. Complete scans of the different blots are presented in Supplementary Fig. 7. (d) Comparison of KUSs and DBeQ for cell death-inducing activities. HeLa cells were treated with 50 μM DBeQ or KUSs for 24 hours.

KUSs and ATP treatments similarly prevented decreases of ATP levels in tunicamycin-treated cells (Fig. 4b). By contrast, KUS11, which could not inhibit VCP ATPase, was unable to prevent the tunicamycin-elicited ATP decrease (Fig. 4b). It is notable that the addition of 0.1 mM ATP or 3 to 10 mM methylpyruvate (weakly membrane-permeable pyruvate, which is converted to ATP in mitochondria) were also ineffective in preventing the aggregation of laminin γ1 (Fig. 4a), but could nevertheless dampen the induction of ER stress, namely CHOP induction (Fig. 4c). These results indicated that the ER is more sensitive to decreases in ATP levels than to the presence of aggregates (see Discussion).

KUSs mitigated pathologies of rd10, a mouse model of retinitis pigmentosa. As we have long been seeking a new strategy to protect retinal neuronal cells, we were intrigued by the observation that VCP was highly expressed in all types of retinal neuronal cells (Supplementary Fig. 3). Furthermore, in retinitis pigmentosa, an involvement of ER stress has been proposed[2,3]. After confirming the neuroprotective efficacy of KUS in retinal organ culture (Supplementary Fig. 4), we then examined whether the protective effects would be observed *in vivo* against the degeneration of photoreceptor cells. For this purpose, rd10 mice were used as a representative mouse model of retinitis pigmentosa[22]. Rd10 mice have a mutation in a gene encoding the rod cyclic guanosine monophosphate (cGMP) phosphodiesterase beta subunit (PDE6B)[22], which is also mutated in patients with retinitis pigmentosa. The mice have been commonly used to test the efficacies of new treatments, including gene therapy, neuroprotectants, and stem cell derived retinal cells.

Starting 7 days after birth, KUS121 or KUS187 was administered daily (50 mg/kg) by intraperitoneal injection. Spectral-domain optical coherence tomography (SD-OCT) examination showed that at age 21 days, the retinas of the control rd10 mice had begun to degenerate (Supplementary Fig. 5a). To test the visual function of the mice, dark-adapted electroretinograms were recorded. The amplitude of the a-wave, which represents visual function of photoreceptors, was smaller in the control mice than in the KUS-treated mice (Supplementary Fig. 5b and c). The peak latency of the a-wave, which negatively correlates with visual function of photoreceptors, was delayed in the control mice as compared with the KUS-treated mice

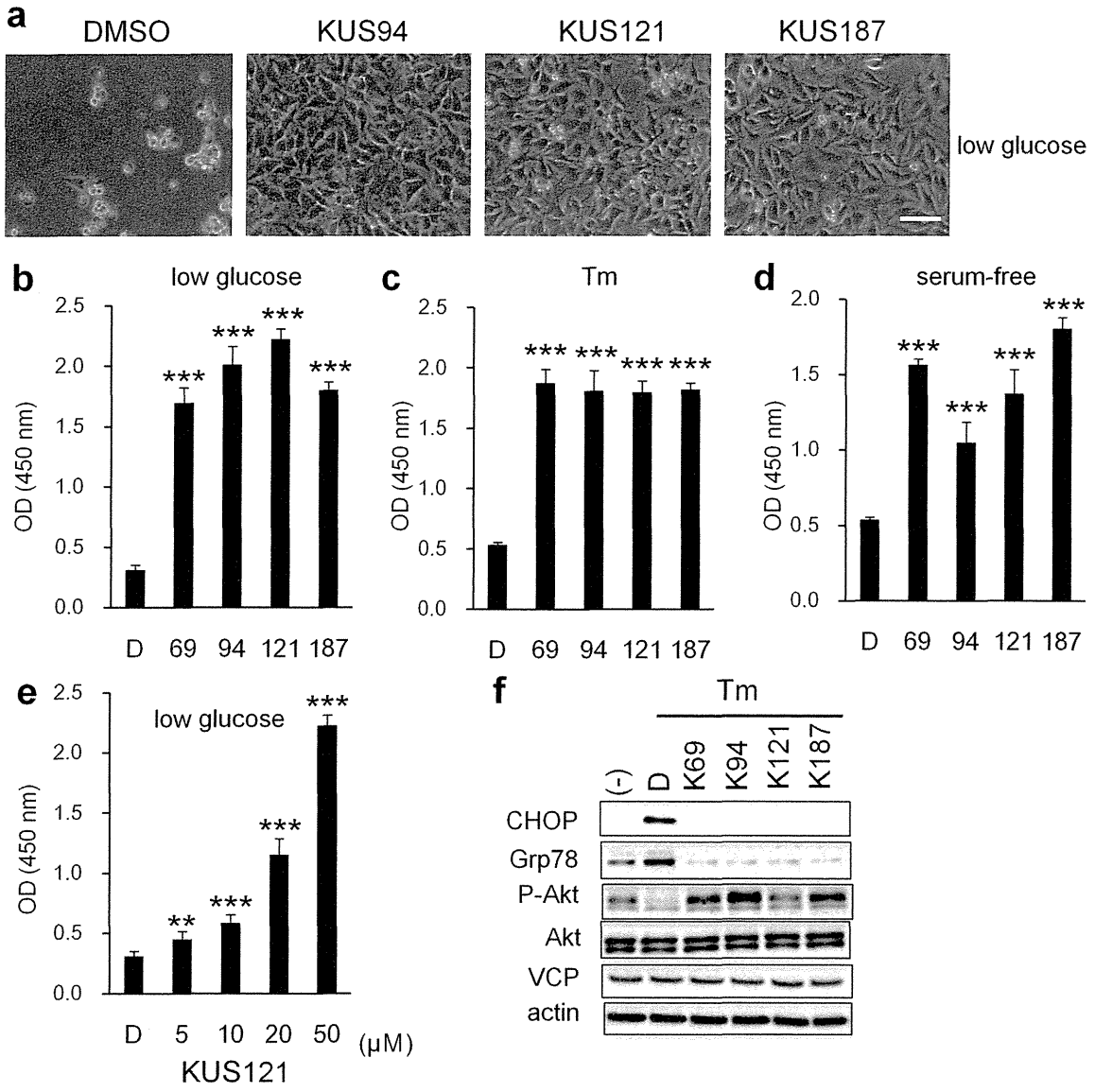

Figure 2 | Prevention of cell death and ER stress by KUSs. (a) Photographs of HeLa cells, cultured with DMSO (DMSO) or KUSs (KUS94, KUS121, and KUS187, 20 μM each) for 41 hours in low glucose (0.2 g/l) medium. Scale bar, 100 μm. (b–e) WST (water-soluble tetrazolium salts) values reflecting relative live cell numbers are shown, as optical density (OD) at 450 nm. Error bars indicate SD. (b) WST values of HeLa cells, cultured in low glucose (0.2 g/l) with DMSO (control) or KUSs (50 μM for KUS121; 20 μM for KUS69, KUS94, and KUS187, n = 3) for 41 hours. (c) Cell viability, indicated by WST values of HeLa cells, cultured with tunicamycin (Tm) (0.2 μg/ml) for 41 hours with KUSs (20 μM each, n = 3). (d) WST values of HEK293 cells, cultured under serum-free conditions for 65 hours with DMSO (control) or KUSs (20 μM each, n = 3). *** $P < 0.001$, vs. DMSO control (Dunnett's test). (e) WST values of HeLa cells, cultured in low glucose (0.2 g/l) medium with different concentrations of KUS121 (5, 10, 20, and 50 μM, n = 3) for 41 hours. ** $P = 0.008$, *** $P < 0.001$, vs. DMSO control (Dunnett's test). (f) Western blot analysis of HeLa cells, treated with tunicamycin (Tm, 0.5 μg/ml) with DMSO (control) or KUSs (50 μM each, KUS69, KUS94, KUS121, and KUS187) for 5 hours. Complete scans of the different blots are presented in Supplementary Fig. 8.

(Supplementary Fig. 5d). At age 25 days, the thinning of the outer nuclear layer (ONL) was clearly observed in the control mice (Fig. 5a). The outer nuclear layer and the junction line between the inner segment and outer segment (arrow heads in Fig. 5a), which is generally considered to be positively associated with visual function[23,24], were clearly detected in the KUS-treated but not in control mice. A very small electroretinogram response was observed in control mice, but an almost normal electroretinogram response was observed in most of the KUS-treated mice (Fig. 5b). At age 29 days, the photoreceptor layer was barely detected in SD-OCT images, and electroretinogram records were almost flat in control mice. In the age-matched KUS-treated mice, the outer nuclear layer, although thin, and an electroretinogram response were still observed (Fig. 5c and d). By histological examination, at age 33 days, the outer nuclear layer in the control mice consisted of only 1–2 rows of cells, but there remained 5–6 rows of cells in the outer nuclear layer in the KUS-treated mice (Fig. 5e). In KUS-treated but not control mice, the outer segment of the photoreceptors was observed (Fig. 5e). The electroretinogram was non-recordable in the control mice, but small b-wave and oscillatory potentials were observed in the KUS-treated mice (Fig. 5f). Time-dependent changes in total retinal thickness measured on SD-OCT images (Fig. 5g) and in b-wave amplitudes of dark-adapted electroretinogram (Fig. 5h) showed that KUS treatments had the potential to prevent or delay the disease progression. b-wave amplitudes of dark-adapted electroretinograms in non-treated wild-type mice mostly remained unchanged or slightly

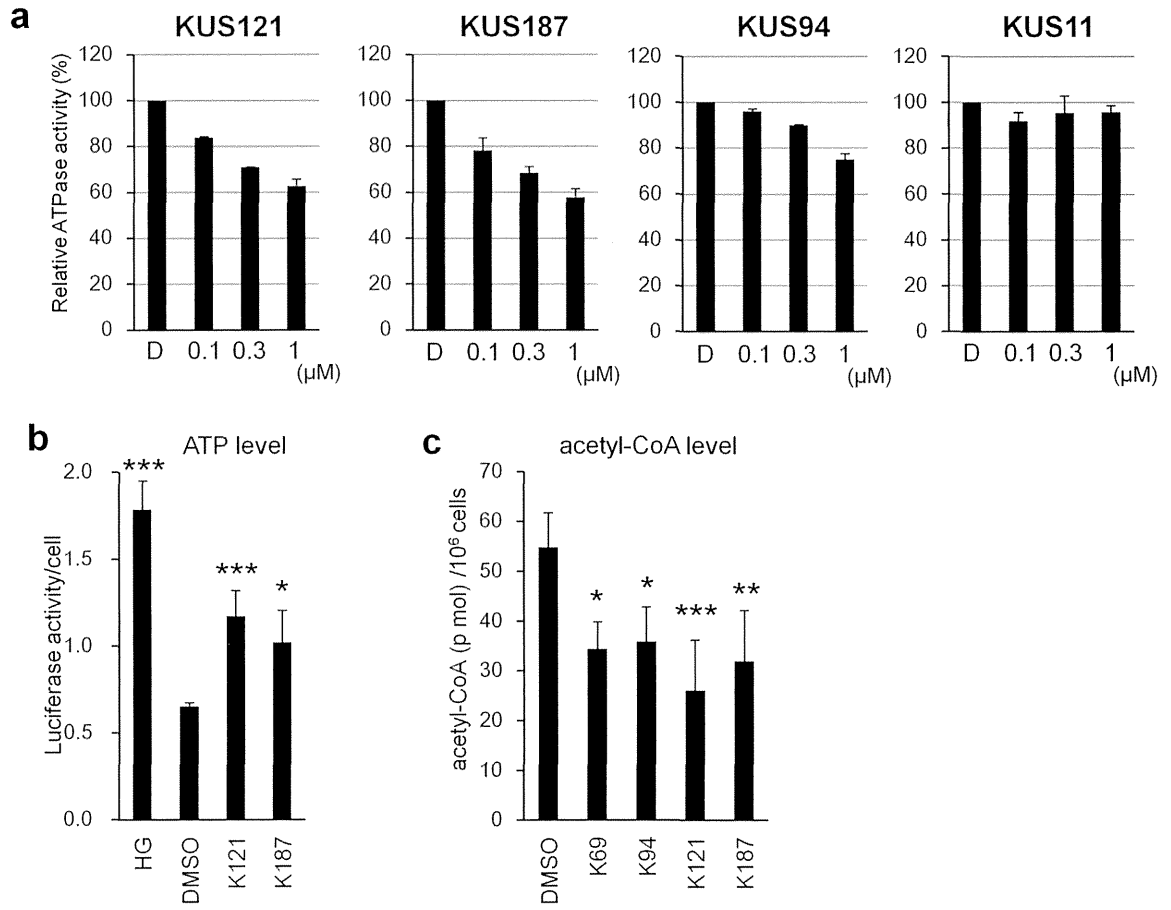

Figure 3 | Effects of KUSs on ATPase activities, ATP levels, and acetyl-CoA levels. (a) Inhibition of ATPase activity in clarified whole cell lysates by KUS121, KUS187, and KUS94, but not KUS11. Total ATPase activities in clarified whole cell lysates from differentiated PC12 cells were measured in the absence and presence of KUSs. Relative ATPase activities are shown with values in the absence of KUS (D: DMSO) set at 100%. (b) HeLa cells were cultured in medium with low glucose (0.25 g/l) for 20 hours, with or without KUSs, and ATP levels were measured with luciferase assays. (c) HeLa cells were cultured in medium with low glucose (0.25 g/l) for 20 hours, with or without KUSs, and acetyl-CoA levels were measured. * $P < 0.05$, ** $P < 0.01$, *** $P < 0.001$ vs. DMSO control (Dunnett's test, n = 3).

increased at the age of 33 days (Supplementary Fig. 6a). Note that KUS administration in adult wild-type mice did not induce any significant change in the amplitude of a- and b-waves (Supplementary Fig. 6b and c). When examined by electron microscopy, the outer segment of the control mouse retina was mostly disarranged at the age of 21 days (Fig. 6a and c), whereas that of KUS-treated mouse retina was regularly arranged (Fig. 6b and d). In rd10 mice, KUS treatments apparently suppressed CHOP expression, as observed in cultured cells (Fig. 5i).

Discussion

We successfully developed novel ATPase inhibitors for VCP, with a naphthalene-derived structure in common, and we collectively called them KUSs (Kyoto University substances). KUSs showed IC_{50} values from 100 nM to 1 μM for the inhibition of ATPase activities of recombinant VCP *in vitro*. Totally different from known ATPase inhibitors for VCP, e.g. DBeQ[14], NMS-873[25], etc., KUSs, e.g. KUS31, KUS69, KUS94, KUS121, KUS187, etc., did not manifest any apparent cellular toxicity, up to 50 μM, on essentially all tested cultured cells; nor did they elicit any aberrant phenotypes that would be expected from the inhibition of cellular VCP functions. These results demonstrated that KUSs could inhibit VCP ATPase activity without inhibiting cellular VCP functions. AAA ATPases might have additional functions that are independent of their ATPase activity. Recently, Noi et al. analyzed the natural movement of recombinant VCP by high-speed atomic force microscopy and demonstrated that ATP-binding mutants of VCP did not display any apparent rotational movement in solution, but wild-type VCP and ATP-hydrolysis mutants of VCP were indistinguishably capable of rotational movements[26]. These data are consistent with the idea that, for at least some VCP functions, ATP binding is essential but ATP hydrolysis is not. This idea is reminiscent of G proteins and actin, whose functions require guanosine triphosphate (GTP) and ATP binding, respectively, but not GTP and ATP hydrolysis, respectively. KUSs likely inhibit the ATPase activity of VCP, but not necessarily VCP functions related to binding of ATP. We thus categorized KUSs as "VCP modulators" rather than "VCP inhibitors".

Surprisingly, KUSs were able to reduce by approximately 40% the total ATP consumption in whole cell soluble lysates of neuronally differentiated PC12 cells, raising the possibility that VCP accounts for approximately 40% of the ATP consumption among soluble ATPases in the non-dividing PC12 cells. This result led us to speculate that KUSs would significantly reduce ATP consumption in living cells as well. Indeed, in cultured cells, KUSs were shown to maintain ATP levels in starved conditions as well as in conditions with enhanced ATP consumption, such as in tunicamycin-induced ER stress[27]. Consistently, and surprisingly, KUSs and ATP similarly suppressed tunicamycin-induced ER stress and eventually cell death. More surprisingly, KUSs (at 50 μM) and ATP (at 0.3 to 1 mM) similarly prevented the aggregation of laminin γ1 in tunicamycin-treated HeLa cells. It is noteworthy that a low level of ATP (at 0.1 mM) and methylpyruvate (at 3 to 10 mM) were not able to

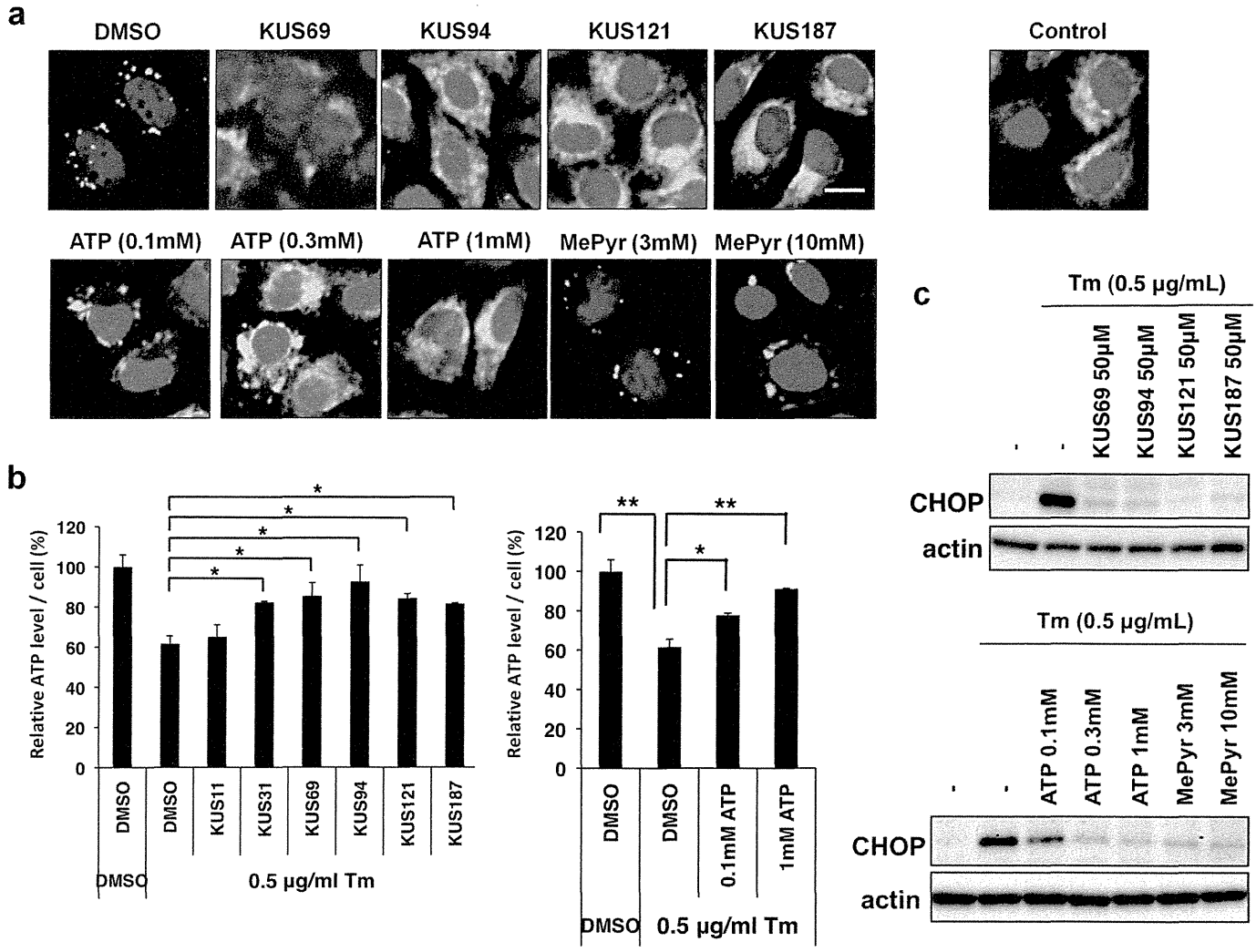

Figure 4 | KUSs and ATP each prevented a decrease of ATP levels and ameliorated ER stress in tunicamycin-treated cells. (a) Immunocytochemical analyses of HeLa cells by an anti-laminin γ1 antibody. HeLa cells were treated with 0.5 μg/ml of tunicamycin (Tm) for 5 hours in the presence of KUSs (50 μM), ATP (0.1, 0.3, and 1 mM), methylpyruvate (MePyr) (3 and 10 mM), or vehicle alone (DMSO). Then, cells were fixed and subjected to immunocytochemical analyses. Normally growing HeLa cells were also analyzed (Control). Scale bar, 10 μm. (b) Measurements of the relative amounts of ATP per cell. HeLa cells were treated with tunicamycin (Tm, 0.5 μg/ml) for 24 hours in the presence of KUSs (50 μM) or ATP (0.1 and 1 mM), or vehicle alone (DMSO), and were harvested. Then, ATP amounts from 1.5×10^5 cells were measured[27]. * $P < 0.05$, ** $P < 0.01$. Error bars indicate SD. (c) Western blot analyses on CHOP. HeLa cells were treated with 0.5 μg/ml of tunicamycin for 5 hours in the presence of KUSs (50 μM), ATP (0.1, 0.3, and 1 mM), methylpyruvate (MePyr) (3 and 10 mM), or vehicle alone (-). Then, cells were harvested and subjected to western blot analyses. Actin served as a loading control. Complete scans of the different blots are presented in Supplementary Fig. 9.

prevent the aggregation of laminin γ1, but were nevertheless able to reduce the induction of CHOP, a well-known ER stress marker, in tunicamycin-treated cells. This observation clearly supports the idea that ER stress is more directly elicited by a decrease of ATP than the presence of aggregated proteins in the ER. Historically, most ER chaperones were originally identified as proteins induced by glucose starvation and thus were named as GRP (glucose-regulated proteins)[28]. Moreover, it has recently been shown that the binding of ER stress sensors, such as PRKR-like endoplasmic reticulum kinase (PERK) and inositol-requiring enzyme-1 (Ire1), to Grp-78 (Bip) is ATP-dependent[29]. Thus, it is likely that a decrease in the ATP level in the ER induces the dissociation of Bip from the ER-stress sensors, leading to their self-oligomerization and subsequent activation.

The evidence that KUSs could prevent the decrease in ATP level in response to several cell death-inducing insults, and eventually cell death, led us to examine the possibility that KUSs would function as cell-protecting compounds in pathological conditions, and that the prevention of early cell death could in turn prevent or delay the deterioration of the affected organs. For this purpose, we chose rd10, a mouse model of retinitis pigmentosa. Currently, it is very difficult to quantitatively measure local ATP levels, and thus we examined whether KUSs could prevent neuronal cell death in the affected retinas.

In rd10 mice, in which the rod cGMP phosphodiesterase beta subunit (PDE6B)[22] is mutated, KUSs significantly retarded the progress of photoreceptor cell death, and protected the photoreceptor cells morphologically as well as functionally. Reduction of ER stress would be a likely mechanism for KUS-mediated protection of photoreceptors, although our current data are not sufficient to exclude other yet-unknown possibilities. In retinitis pigmentosa, neuroprotective treatment is regarded as an important future therapeutic strategy, and several clinical trials to prolong the viability of the retinal neuronal cells have been ongoing[1]. We are also planning to initiate clinical studies using KUSs in the near future.

Considering all of the data together, we posit that a reduction of ATP levels is a common condition in the affected organs of incurable

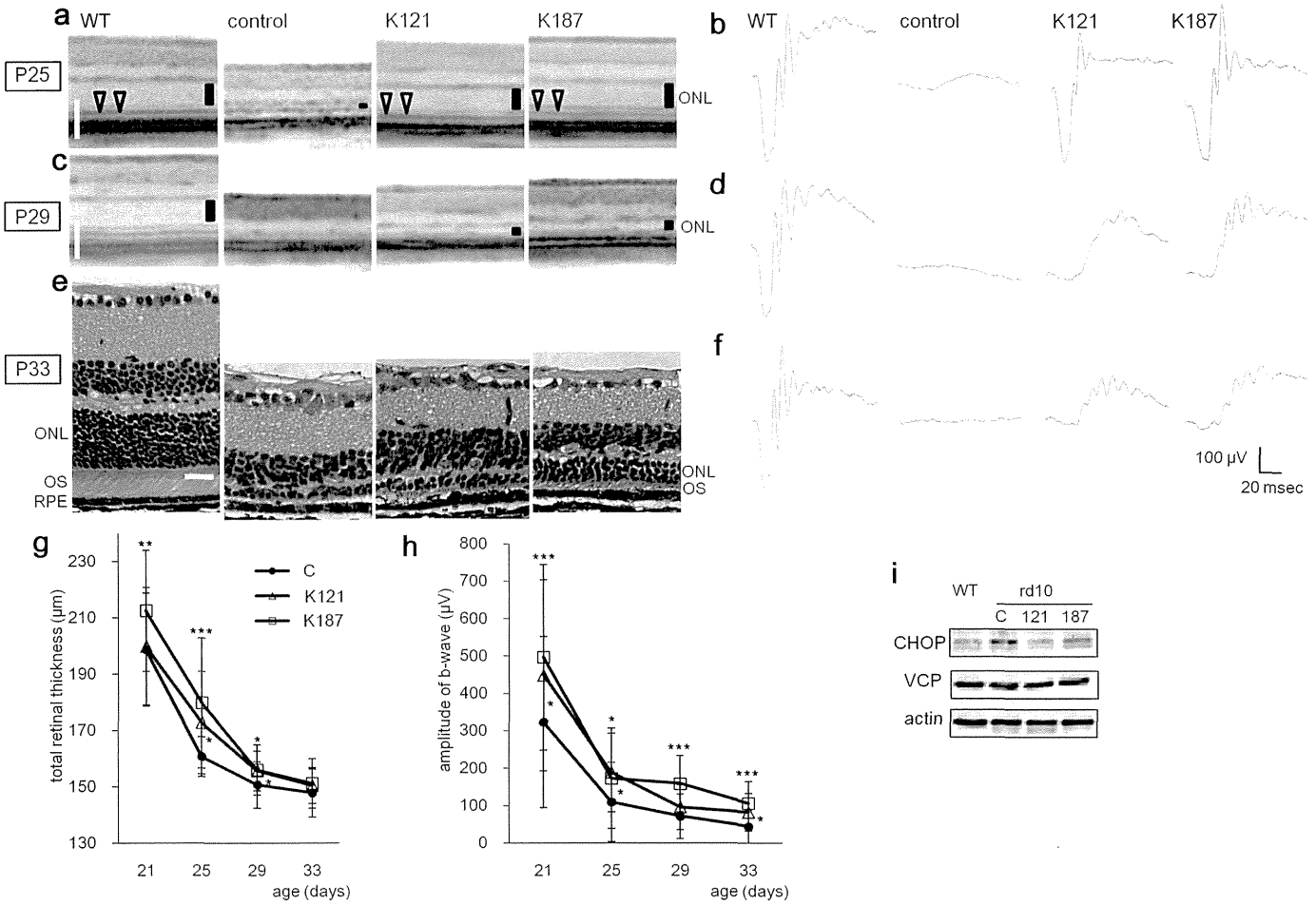

Figure 5 | *in vivo* efficacies of KUSs in the rd10 mouse model of retinitis pigmentosa. (a, c) Representative live sectional images (vertical sections) by SD-OCT of retinas in 25- (a) and 29-day-old (c) normal C57BL/6 mouse (WT) and rd10 mice, administered KUS 121 (n = 17), KUS187 (n = 21), or saline (n = 18) as a control. Vertical bars in the images indicate the thickness of outer nuclear layer (ONL). Note that the ONL was barely detectable in saline-treated control rd10 mice. (b, d, f) Electroretinogram of 25- (b), 29- (d) and 33-day-old (f) normal C57BL/6 mouse (WT) and rd10 mice, administered KUSs or saline. (e) HE-stained retinas of 33-day-old normal C57BL/6 mouse (WT) and rd10 mice, administered KUSs or saline. RPE: retinal pigment epithelium. OS: outer segment. Scale bars (shown by white color), 100 μm in (a) and (c); 20 μm in (e). (g, h) Time-dependent changes of total retinal thickness (g) and b-wave amplitude in dark-adapted electroretinogram (h) in rd10 mice administered KUSs or saline. * $P < 0.05$, ** $P < 0.01$, *** $P < 0.005$ vs. saline (Dunnett's test). Error bars indicate SD. (i) Western blot analysis of dissected retinas of 21-day-old rd10 mice administered KUSs or saline. WT: C57BL/6 control mice. Complete scans of the different blots are presented in Supplementary Fig. 10.

disorders with early cell death. Because many proteins require ATP, a reduction of ATP levels would contribute to a functional decline in affected cells or organs in early stages of the disease, which might precede cell death. Reducing ATP consumption by way of KUSs and/or enhancing ATP generation by yet-unknown compounds would be a novel strategy to retard these processes and thus to prevent or retard the progression of clinical manifestations. Recently, the involvement of translational suppression via phosphorylation of eIF2α has been proposed in the pathogenesis of Alzheimer[30] and prion diseases[31]. Indeed, novel PERK inhibitors showed significant efficacies in a mouse prion disease model[32]. Given that PERK is the kinase responsible for the phosphorylation of eIF2α in ER stress, the effect of KUSs in these disease models would be worth evaluating.

In conclusion, we showed that KUSs, new compounds developed as ATPase inhibitors of VCP, have novel functions as "VCP modulators" or "ATP regulators" without apparent inhibition of cellular VCP functions. These new "ATP regulators" have strong neuroprotective effects *in vivo* on retinal photoreceptor cells. The efficacies were apparently correlated with their abilities to suppress ER stress. To the best of our knowledge, KUSs are the first small chemicals that can prevent cell death in an animal model of human retinitis pigmentosa. Given that the major pathology of many other incurable human disorders, e.g. neurodegenerative diseases, ischemic diseases, etc., is also early cell death, KUSs may provide a novel strategy for cell protection in such incurable disorders.

Methods

Cell culture. HeLa, HEK293, and PC12 cells were cultured in Dulbecco's modified Eagle's medium (DMEM) with 10% fetal bovine serum. Tunicamycin (0.2–2 μg/ml, Nacalai Tesque, Kyoto, Japan) was added to induce ER stress. Viability of cultured cells was measured by formazan production with an ARVO multilabel counter (Wallac), using WST (water soluble tetrazolium salts)-8 reagent (Cell count reagent SF, Nacalai Tesque, Kyoto, Japan). ATP in cultured cells was measured by luciferase activities with an ARVO multilabel counter, using ATP assay reagent for cells (Toyo B-net, Tokyo, Japan). Acetyl-CoA was measured using a PicoProbe Acetyl CoA assay kit (BioVision, CA, USA) with a Spectra Max multilabel counter (Molecular Devices, CA, USA).

Measurement of ATPase activities. We measured ATPase activities by modifying the molybdate assay, which was as described previously[8]. In the assay, 1 μg of whole cell soluble lysate of neuronally differentiated PC12 cells, or 500 ng recombinant VCP protein, was incubated in 20 μl of the ATPase assay buffer (20 mM HEPES (pH 7.4), 50 mM KCl, 5 mM $MgCl_2$) with 100 μM [γ-^{32}P]ATP (18.5 GBq/mmol) (PerkinElmer) at 37°C for 20 min. After incubation, the reaction was quenched by addition of 200 μl of 8% ice-cold trichloroacetic acid solution with 1 mM K_2HPO_4,

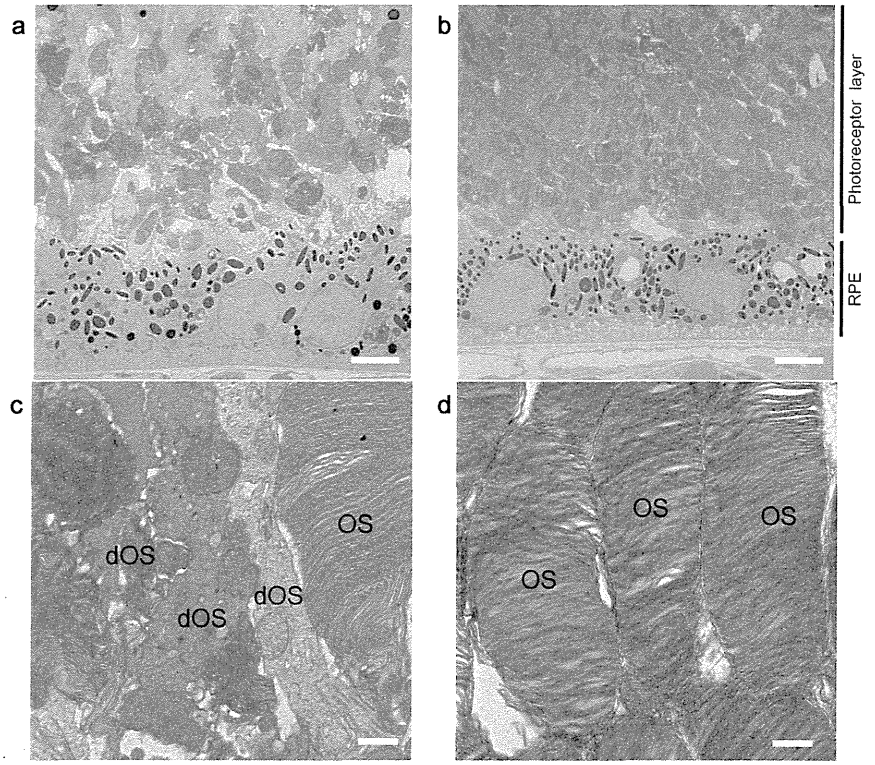

Figure 6 | KUSs preserved retinal microstructures in the rd10 mouse model of retinitis pigmentosa. Electron micrographs of 21-day-old rd10 mice, administered saline (a, c) or KUS187 (b, d). RPE, retinal pigment epithelium. Note that morphologies of outer segments of retinas in KUS-treated rd10 mice were well preserved but most of the outer segments in saline-treated control rd10 mice were degenerated. OS in (c) and (d) indicates morphologically intact outer segment, and dOS in (c) morphologically degenerated outer segment. Scale bars: 5 μm in (a) and (b); 500 nm in (c) and (d).

and then 50 μl of solution A (3.75% ammonium molybdate, 0.02 M silicotungstic acid in 3 N H_2SO_4) and 300 μl of *n*-butyl acetate were added to the reaction. The samples were mixed well and centrifuged at 12,000 × g for 1 min. Then, 200 μl aliquots from the upper organic phases were taken and their radioactivity was determined with a liquid scintillation counter for β-radiation, which determined the amounts of ^{32}P released.

Antibodies. Polyclonal antibodies against VCP were developed in our laboratory as described previously[12]. Anti-Grp78, anti-Akt and anti-phospho-Akt (Ser 473) antibodies were purchased from Cell Signaling (MA, USA); anti-tubulin, anti-CHOP and anti-laminin γ1 from Santa Cruz Biotechnology (CA, USA); anti-actin from Chemicon (MA, USA); anti-ubiquitin from Millipore (MA, USA), and anti-LC3 from MBL (Nagoya, Japan).

Animal experiments. Animal experiments were conducted in accordance with the Association Research in Vision and Ophthalmology (ARVO) Statement for the Use of Animals in Ophthalmic and Vision Research. All protocols were approved by the Institutional Review Board of the Kyoto University Graduate School of Medicine (MedKyo11229). Rd10 mice[22] were obtained from the Jackson Laboratory (Bar Harbor, ME, USA). The environment was maintained at a 14-hour light/10-hour dark cycle. All mice were fed ad libitum. Before image acquisition or electroretinogram examination, the mice were anesthetized by an intraperitoneal injection of pentobarbital (50 mg/kg body weight). Pupils were dilated to approximately 2 mm in diameter using tropicamide and phenylephrine (0.5% each) eye drops.

SD-OCT image acquisition and measurement of retinal thickness. Spectral-domain optical coherence tomography (SD-OCT) examinations using *Multiline OCT* (Heidelberg Engineering, Heidelberg, Germany) were performed[33] in rd10 mice at ages of 21, 25, 29, and 33 days. Total retinal thickness (from inner limiting membrane to Bruch membrane) in rd10 mice was measured using volume scan images[33] within a circle 0.366 mm in diameter, the center of which was adjusted to the center of the optic nerve head. The mean value of the upper and lower quadrant was averaged.

Electroretinogram. Electroretinogram recording was performed to assess the visual function of rd10 mice at ages of 21, 25, 29, and 33 days. Mice were dark-adapted overnight before anesthetization. Electroretinograms were recorded using a gold loop corneal electrode with a light-emitting diode (Mayo Corp., Inazawa, Japan). A reference electrode was placed in the mouth and a ground electrode was inserted to the anus. Stimuli were produced with a light emitting diode stimulator (Mayo Corp.). The electroretinogram response signals were amplified, digitized at 10 kHz with a band-pass filter of 0.3 to 500 Hz, and analyzed (PowerLab 2/25; AD instruments, New South Wales, Australia). The a- and b-wave amplitudes and a-wave latency of the mixed cone and rod response (ISCEV (International Society for Clinical Electrophysiology of Vision) standard; scotopic 3.0)[34] were analyzed.

Histological analyses. The eyes were fixed in 4% paraformaldehyde for 24 hours at 4°C and embedded in paraffin. Serial 6-μm paraffin-embedded sections that passed through the center of the optic nerve head were selected. The selected retinal sections were stained with hematoxylin-eosin (HE) and photographed about 400 μm apart from the center of the optic nerve head under an optical microscope (Axioplan 2; Carl Zeiss Jena GmbH, Jena, Germany). For electron microscopic examination, eyes were fixed overnight in a mixture of 10% neutral buffered formalin and 2.5% glutaraldehyde for 2.5 hours and subsequently fixed in 1% osmium tetroxide for 90 min. The retina was dehydrated through a graded series of ethanol (50–100%), cleared in propylene oxide, and embedded in epoxy resin. Ultrathin sections were cut by using an ultramicrotome and stained with uranyl acetate and lead citrate. The stained sections were observed by transmission electron microscopy (H-7650, Hitachi Co., Tokyo, Japan).

Statistical analysis. Variables among cells or mice treated with or without KUSs were compared with Dunnett's test or Student's *t*-test. Statistical analyses were performed using PASW Statistics version 17.0 (SPSS Inc., Chicago, IL). The level of statistical significance was set at $P < 0.05$.

1. Birch, D. G., Weleber, R. G., Duncan, J. L., Jaffe, G. J. & Tao, W. Randomized trial of ciliary neurotrophic factor delivered by encapsulated cell intraocular implants for retinitis pigmentosa. *Am. J. Ophthalmol.* **156**, 283–292 (2013).
2. Lin, J. H. & Lavail, M. M. Misfolded proteins and retinal dystrophies. *Adv. Exp. Med. Biol.* **664**, 115–121 (2010).
3. Jiang, H., Xiong, S. & Xia, X. Retinitis pigmentosa-associated rhodopsin mutant T17M induces endoplasmic reticulum (ER) stress and sensitizes cells to ER stress-induced cell death. *Mol. Med. Rep.* **9**, 1737–1742 (2014).
4. Higashiyama, H. *et al.* Identification of *ter94*, *Drosophila VCP*, as a modulator of polyglutamine-induced neurodegeneration. *Cell Death Differ.* **9**, 264–273 (2002).
5. Kakizuka, A. Roles of VCP in human neurodegenerative disorders. *Biochem. Soc. Trans.* **36**, 105–108 (2008).
6. Watts, G. D. *et al.* Inclusion body myopathy associated with Paget disease of bone and frontotemporal dementia is caused by mutant valosin-containing protein. *Nat. Genet.* **36**, 377–381 (2004).

7. Johnson, J. O. *et al.* Exome sequencing reveals *VCP* mutations as a cause of familial ALS. *Neuron* **68**, 857–864 (2010).
8. Manno, A., Noguchi, M., Fukushi, J., Motohashi, Y. & Kakizuka, A. Enhanced ATPase activities as a primary defect of mutant valosin-containing proteins that cause inclusion body myopathy associated with Paget disease of bone and frontotemporal dementia. *Genes Cells* **15**, 911–922 (2010).
9. Stolz, A., Hilt, W., Buchberger, A. & Wolf, D. H. Cdc48: a power machine in protein degradation. *Trends Biochem. Sci.* **36**, 515–523 (2011).
10. Meyer, H., Bug, M. & Bremer, S. Emerging functions of the VCP/p97 AAA-ATPase in the ubiquitin system. *Nat. Cell Biol.* **14**, 117–123 (2012).
11. Wolf, D. H. & Stolz, A. The Cdc48 machine in endoplasmic reticulum associated protein degradation. *Biochim. Biophys. Acta.* **1823**, 117–124 (2012).
12. Hirabayashi, M. *et al.* VCP/p97 in abnormal protein aggregates, cytoplasmic vacuoles, and cell death, phenotypes relevant to neurodegeneration. *Cell Death Differ.* **8**, 977–984 (2001).
13. Kobayashi, T., Tanaka, K., Inoue, K. & Kakizuka, A. Functional ATPase activity of p97/valosin-containing protein (VCP) is required for the quality control of endoplasmic reticulum in neuronally differentiated mammalian PC12 cells. *J. Biol. Chem.* **277**, 47358–47365 (2002).
14. Chou, T. F. *et al.* Reversible inhibitor of p97, DBeQ, impairs both ubiquitin-dependent and autophagic protein clearance pathways. *Proc. Natl. Acad. Sci. USA* **108**, 4834–4839 (2011).
15. Zinszner, H. *et al.* CHOP is implicated in programmed cell death in response to impaired function of the endoplasmic reticulum. *Genes Dev.* **12**, 982–995 (1998).
16. Kim, R., Emi, M., Tanabe, K. & Murakami, S. Role of the unfolded protein response in cell death. *Apoptosis* **11**, 5–13 (2006).
17. Franke, T. F., Kaplan, D. R. & Cantley, L. C. PI3K: downstream AKTion blocks apoptosis. *Cell* **88**, 435–437 (1997).
18. Yi, C. H. *et al.* Metabolic regulation of protein N-α-acetylation by Bcl-xL promotes cell survival. *Cell* **146**, 607–620 (2011).
19. Naidoo, N. ER and aging-Protein folding and the ER stress response. *Ageing Res. Rev.* **8**, 150–159 (2009).
20. Gardner, B. M., Pincus, D., Gotthardt, K., Gallagher, C. M. & Walter, P. Endoplasmic reticulum stress sensing in the unfolded protein response. *Cold Spring Harb. Perspect. Biol.* **5**, a013169 (2013).
21. Gorman, A. M., Healy, S. J. M., Jager, R. & Samali, A. Stress management at the ER: regulators of ER stress-induced apoptosis. *Pharmacol. Ther.* **134**, 306–316 (2012).
22. Chang, B. *et al.* Retinal degeneration mutants in the mouse. *Vision Res.* **42**, 517–525 (2002).
23. Ojima, Y. *et al.* Restoration of outer segments of foveal photoreceptors after resolution of central serous chorioretinopathy. *Jpn. J. Ophthalmol.* **54**, 55–60 (2010).
24. Oishi, A. *et al.* The significance of external limiting membrane status for visual acuity in age-related macular degeneration. *Am. J. Ophthalmol.* **150**, 27–32 (2010).
25. Magnaghi, P. *et al.* Covalent and allosteric inhibitors of the ATPase VCP/p97 induce cancer cell death. *Nat. Chem. Biol.* **9**, 548–556 (2013).
26. Noi, K. *et al.* High-speed atomic force microscopic observation of ATP-dependent rotation of the AAA+ chaperone p97. *Structure* **21**, 1992–2002 (2013).
27. Okamoto, A., Koike, M., Yasuda, K. & Kakizuka, A. Maintaining ATP levels via the suppression of PERK-mediated rRNA synthesis at ER stress. *Biochem. Biophys. Res. Commun.* **394**, 42–47 (2010).
28. Lee, A. S. The glucose-regulated proteins: stress induction and clinical applications. *Trends Biochem. Sci.* **26**, 504–510 (2001).
29. Sou, S. N., Ilieva, K. M. & Polizzi, K. M. Binding of human BiP to the ER stress transducers IRE1 and PERK requires ATP. *Biochem. Biophys. Res. Commun.* **420**, 473–478 (2012).
30. Ma, T. *et al.* Suppression of eIF2α kinases alleviates Alzheimer's disease-related plasticity and memory deficits. *Nat. Neurosci.* **16**, 1299–1305 (2013).
31. Moreno, J. A. *et al.* Sustained translational repression by eIF2α-P mediates prion neurodegeneration. *Nature* **485**, 507–511 (2012).
32. Moreno, J. A. *et al.* Oral treatment targeting the unfolded protein response prevents neurodegeneration and clinical disease in prion-infected mice. *Sci. Transl. Med.* **5**, 206ra138 (2013).
33. Muraoka, Y. *et al.* Real-time imaging of rabbit retina with retinal degeneration by using spectral-domain optical coherence tomography. *PloS One* **7**, e36135 (2012).
34. Marmor, M. F. *et al.* ISCEV Standard for full-field clinical electroretinography (2008 update). *Doc. Ophthalmol.* **118**, 69–77 (2009).

Acknowledgments

We thank Michiko Tsuji, Yuri Terado, Noriko Suzuki, Keiko Kuroiwa, Masami Suetsugu, and Kaori Misonou for their technical assistance; Gerhard Zinser of Heidelberg Engineering for discussion on the *Multiline* OCT; and members of Kakizuka Lab for discussion. We also thank Professor James A. Hejna (Kyoto University) for critical reading of the manuscript. This research was supported in part by Research grants from the Astellas Foundation for Research on Metabolic Disorders, the Japan Foundation for Applied Enzymology, the Uehara Memorial Foundation, Mochida Memorial Foundation for Medical and Pharmaceutical Research, YOKOYAMA Foundation for Clinical Pharmacology (YRY1308), Japan Intractable Diseases Research Foundation, Japan Research Foundation for Clinical Pharmacology (I.O.H.), and a Grant-in-Aid for Young Scientists (24791850) and grants from SORST of JST (A.K.), the Ministry of Education, Culture, Sports, Science, and Technology of Japan (A.K., I.O.H. and N.Y.), and the Ministry of Health, Labour, and Welfare of Japan (A.K., I.O.H. and N.Y.).

Author contributions

H.O.I. designed and conducted the majority of the animal experiments, and prepared the manuscript. N.S., M.K., S.H. and A.I. conducted experiments with cultured cells. N.N. conducted mouse experiments. Y.M. conducted some of the mouse experiments and electron microscopic examination. Y.T. made histological sections. T.F. and T.S. developed KUSs. N.Y. helped with experimental design. A.K. conceived the project and helped with writing the manuscript. All authors discussed the results and commented on the manuscript.

Additional information

Supplementary information accompanies this paper at http://www.nature.com/scientificreports

Competing financial interests: Yes, there is potential Competing Interest. In relation to this manuscript, Kyoto University and Daito Chemix applied for patents (PCT/JP2011/067320 & PCT/JP2011/073160), and Hanako Ohashi Ikeda, Noriko Nakano, Tomohiro Fuchigami, Toshiyuki Shudo, Seiji Hori, Nagahisa Yoshimura & Akira Kakizuka were inventors of the applied patents. The other authors declare no competing interests.

How to cite this article: Ikeda, H.O. *et al.* Novel VCP modulators mitigate major pathologies of rd10, a mouse model of retinitis pigmentosa. *Sci. Rep.* **4**, 5970; DOI:10.1038/srep05970 (2014).